A theoretical study of P4O6: Vibrational analysis and infrared and Raman spectra

ARTICLE *in* JOURNAL OF MOLECULAR STRUCTURE THEOCHEM · OCTOBER 2000

Impact Factor: 1.37 · DOI: 10.1016/S0166-1280(00)00465-6

ELSEVIER

Journal of Molecular Structure (Theochem) 531 (2000) 323–331

THEO CHEM

www.elsevier.nl/locate/theochem

A theoretical study of P_4O_6: vibrational analysis and infrared and Raman spectra

J.O. Jensen[a], A. Banerjee[a], C.N. Merrow[b], D. Zeroka[c,*], J. Michael Lochner[a]

[a]*US Army Edgewood Chemical and Biological Center, Aberdeen Proving Ground, MD 21010-5423, USA*
[b]*Department of Chemistry, University of Missouri at Rolla, Rolla, MO 65409, USA*
[c]*Department of Chemistry, Lehigh University, Bethlehem, PA 18015-3172, USA*

Received 21 February 2000; accepted 1 March 2000

Abstract

The normal mode frequencies and the corresponding vibrational assignments of tetraphosphorus hexoxide (P_4O_6) in T_d symmetry are examined theoretically using the GAUSSIAN 94 set of quantum chemistry codes at the HF/6-31G*, MP2/6-31G* and DFT/B3LYP/6-31G* levels of theory. By comparison to experimental normal mode frequencies deduced by Chapman [A.C. Chapman, Spectrochim. Acta A 24 (1968) 1687–1696] correction factors for predominant vibrational motions are determined and compared. Normal modes were decomposed into three nonredundant motions {P–O–P wag, P–O–P bend, and P–O stretch}. Standard deviations found for the DFT and MP2 corrected frequencies compared to experiment are particularly noteworthy yielding values of 15 and 11 cm^{-1}, respectively.

Keywords: Vibrations; Normal mode frequencies; Infrared spectra; Raman spectra; Tetraphosphorus hexoxide

1. Introduction

The oxidation of elemental phosphorus has been an important but mechanistically illusive chemical reaction since its investigation by Boyle over 300 years ago. Several different molecules are produced during oxidation, due to the multiple oxidation states available to phosphorus and due to the strength of the bridging and terminal oxygen bonds. While the oxidation reaction is not spontaneous, it is extremely exothermic. The reactions of oxygen atoms with phosphorus compounds are among the most intense chemiluminescent reactions and thus form the basis of a possible laser system [1–5]. A featureless continuum extending from 360 nm to the infrared has been generally observed over a wide range of reaction conditions. Hamilton and Murrells [6] have studied the reaction intermediates of the phosphorus oxidation using a discharge-flow/mass spectrometry technique. Two kinetically distinct emissions were observed:

- for O in excess, an intense white-green emission extending down to 360 nm is due to the reaction $O + PO \rightarrow PO_2 + h\nu$;
- while for an O-scarce environment, the blue emission is assigned to the reaction $O + POH \rightarrow PO_2 + h\nu$.

The Group 5 oxides are introduced in many chemistry textbooks as prototype examples of cage inorganic structures and serve as molecular "models" for

* Corresponding author. Tel.: + 1-610-758-3479; fax: + 1-610-758-6536.

E-mail addresses: jojensen@sbccom.apgea.army.mil (J.O. Jensen); axbanerj@c-mail.apgea.army.mil (A. Banerjee); merrow@umr.edu (C.N. Merrow); dz00@lehigh.edu (D. Zeroka); jmlochne@sbccom.apgea.army.mil (J. Michael Lochner).

0166-1280/00/$ - see front matter
PII: S0166-1280(00)00465-6

Table 1
Calculated geometries for the ground electronic state of P_4O_6 in T_d symmetry at three levels of calculation; for comparison the experimental geometrical coordinates deduced from electron diffraction of P_4O_6 in the vapor phase are also listed

Geometrical coordinate	HF/6-31G*	MP2/6-31G*	DFT/B3LYP/6-31G*	Experimental[ab]	Experimental[c]
r(P–O) (pm)	164	166	167	165 ± 2	163.8 ± 0.3
∠P–O–P (°)	129.5	127.8	127.9	127.5 ± 1	126.4 ± 0.7
∠O–P–O (°)	97.9	98.9	98.9	99 ± 1	99.8 ± 0.8

[a] Ref. [15].
[b] Ref. [16].
[c] Ref. [17].

solid-state systems. The oxides can be thought of as obtained by adding oxygen atoms to the parent-element tetrahedron (M_4: M = P, As, Sb). An interesting feature of the molecules containing the third row atoms is the extent to which the formally empty 3d orbitals participate in bonding. This is particularly relevant in the case of phosphorus compounds [7].

Our interest is in building detectors of P-containing and S-containing compounds in the interest of, for example, treaty violations, etc. where phosphorus oxides are abundant reaction products. We therefore are interested in the mechanism of chemiluminiscence and their reaction mechanisms. Calculations of electronic ground state properties and vibrational modes are the first step.

In this report we focus on the cage molecule P_4O_6,

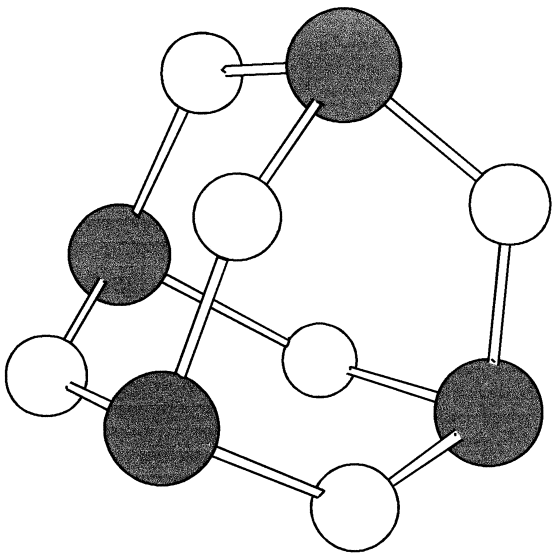

Fig. 1. Optimized geometry for P_4O_6.

which is historically named phosphorus trioxide but correctly named tetraphosphorus hexoxide. Relevant previous studies on P_4O_6 include infrared and Raman spectroscopic studies [8–10] at room temperature in which vibrational assignments were made. In addition some ab initio electronic structure studies [11–13] have examined electronic energies. An ab initio electronic structure study [14] has been performed to determine infrared and Raman spectral parameters of P_4O_6. Structural geometrical parameters have been deduced from electron diffraction studies [15–17] on vapor phase P_4O_6.

2. Computational details

The structure and the vibrational frequencies of P_4O_6 at the Hartree–Fock (HF) [18], second-order Møller–Plesset (MP2) [19], and Density Functional Theory (DFT) using the exchange correlation function B3LYP [20,21] levels of theory are calculated using the standard 6-31G* basis set. All calculations are performed using the GAUSSIAN 94 Program Package [22] running on a four processor SGI O200 and the SGI Origin 2000 computers at the Army Research Laboratory High Performance Computing Center.

The optimized structure of P_4O_6, in T_d symmetry, at each level of theory is reported in Table 1. The calculations utilized the T_d symmetry of the P_4O_6 molecule. The optimized structure, corresponding to each of the three levels of theory that are considered, is displayed in Fig. 1. As can be seen from the results in Table 1 each of the three levels of theory predict geometrical coordinates in close accord with experiment [15–17] with the MP2 results being very slightly superior to the HF or DFT results.

Table 2
IR spectral analysis for the T_d form of P_4O_6 performed at the HF/6-31G* level of theory (all frequencies in units of cm^{-1})

Symmetry	Frequency no.	Computed frequency	Experimental frequency[a]	IR intensity[b]	Raman intensity[c]	Assignment	Corrected frequency
A_1	ν_1	825	718	IR inactive	1	P–O–P bend	714
	ν_2	681	613		19	P–O stretch	598
E	ν_3	699	643	IR inactive	2	P–O stretch	614
	ν_4	332	285		2	P–O–P bend	287
T_1	ν_5	723	569	IR inactive	R inactive	P–O stretch	635
	ν_6	332	302			P–O–P wag	299
T_2	ν_7	1069	919	1041	4	P–O stretch	939
	ν_8	695	643	111	6	P–O stretch	610
	ν_9	634	549	0	0	P–O–P bend	548
	ν_{10}	458	407	2	2	P–O–P wag	412
						σ	26

[a] Experimental frequencies [9] determined from the infrared spectrum of a liquid solution of P_4O_6 in CS_2 and the Raman spectrum of liquid P_4O_6. The symmetry assignments used for some of the experimental frequencies in this table differ from those used in the Chapman article. In addition assignments agree with those made by Mowrey et al. [14] with the exception of 643 cm^{-1} (E) and 569 cm^{-1} (T_1) where Mowrey et al. used 691 cm^{-1} (E) and 702 cm^{-1} (T_1).

[b] Units of IR activity are km/mol.

[c] Units of Raman scattering activity are $Å^4$/amu.

Table 3
IR spectral analysis for the T_d form of P_4O_6 performed at the MP2/6-31G* level of theory (all frequencies in units of cm^{-1})

Symmetry	Frequency no.	Computed frequency	Experimental frequency[a]	IR intensity[b]	Assignment	Corrected frequency
A_1	ν_1	739	718	IR inactive	P–O–P bend	738
	ν_2	616	613		P–O stretch	600
E	ν_3	648	643	IR inactive	P–O stretch	632
	ν_4	292	302		P–O–P bend	292
T_1	ν_5	606	569	IR inactive	P–O stretch	591
	ν_6	286	302		P–O–P wag	285
T_2	ν_7	971	919	844	P–O stretch	946
	ν_8	643	643	85	P–O stretch	627
	ν_9	555	549	2	P–O–P bend	554
	ν_{10}	409	407	39	P–O–P wag	407
					σ	15

[a] Experimental frequencies [9] determined from the infrared spectrum of a liquid solution of P_4O_6 in CS_2 and the Raman spectrum of liquid P_4O_6. The symmetry assignments used for some of the experimental frequencies in this table differ from those used in the Chapman article. In addition assignments agree with those made by Mowrey et al. [14] with the exception of 643 cm^{-1} (E) and 569 cm^{-1} (T_1) where Mowrey et al. used 691 cm^{-1} (E) and 702 cm^{-1} (T_1).
[b] Units of IR activity are km/mol.

The vibrational frequencies of P_4O_6 were calculated at the Hartree–Fock, MP2, and DFT/B3LYP levels of theory using the standard 6-31G* basis set. Each of the vibrational modes was assigned to one of three types of motion {P–O–P wag, P–O–P bend, and P–O stretch} by means of visual inspection using the AVS-Chemistry-Viewer [23] set of programs or the GaussView [24] visualization program.

The high degree of symmetry for an isolated molecule of P_4O_6 is very helpful in making vibrational assignments. The assignments are determined by using standard procedures whereby the traces of the symmetry operations are decomposed into the irreducible representations of the T_d point group [25]. Our symmetry analysis for the vibrational modes of P_4O_6 is presented in some detail in order to describe the basis for our assignments.

The fundamental vibrations of the P_4O_6 are representable as the following decomposition in terms of irreducible representations of a representation Γ:

$$\Gamma = 2A_1 + 2E + 2T_1 + 4T_2$$

- P–O stretching modes: the 12 P–O single bonds form the basis of our analysis. Each σ_d operator has a trace of 2. All other operators except E have a trace of 0. Thus the symmetries are A_1, E, T_1, and 2-T_2.
- P–O–P bending modes: the six P–O–P bending motions are the basis of our analysis. Each C_2 operator has a trace of 2 and the σ_d operator has a trace of 2. All other operators, except E, have a trace of 0. Thus the symmetries are A_1, E, and T_2.
- P–O–P wagging modes: the six P–O–P motions that are perpendicular to the P–O–P bond angle form the basis of our analysis. Each C_2 operator has a trace of -2. All other operators except E have a trace of 0. Thus the symmetries are T_1 and T_2.

For each of the vibrational modes assigned, one of the three motions {P–O stretch, P–O–P bend and P–O–P wag} is visually assigned using the AVS-Chemistry-Viewer [23] and the GaussView [24] visualization programs. The choice of internal coordinates is always somewhat arbitrary. However, we have found the above set to be complete and nonredundant. Other redundant coordinates, e.g. the O–P–O bending motion, can be completely determined using the set of three motions given above.

By combining the results from the AVS-Chemistry-Viewer [23] and the GaussView [24] visualization programs with the symmetry considerations and our

Table 4
IR spectral analysis for the T_d form of P_4O_6 performed at the DFT/B3LYP/6-31G* level of theory (all frequencies in units of cm^{-1})

Symmetry	Frequency no.	Computed frequency	Experimental frequency[a]	IR intensity[b]	Assignment	Corrected frequency
A_1	ν_1	725	718	IR inactive	P–O–P bend	737
	ν_2	596	613		P–O stretch	609
E	ν_3	625	643	IR inactive	P–O stretch	638
	ν_4	289	302		P–O–P bend	294
T_1	ν_5	559	569	IR inactive	P–O stretch	571
	ν_6	279	285		P–O–P wag	285
T_2	ν_7	925	919	770	P–O stretch	945
	ν_8	620	643	82	P–O stretch	633
	ν_9	542	549	3	P–O–P bend	551
	ν_{10}	398	407	32	P–O–P wag	407
					σ	11

[a] Experimental frequencies [9] determined from the infrared spectrum of a liquid solution of P_4O_6 in CS_2 and the Raman spectrum of liquid P_4O_6. The symmetry assignments used for some of the experimental frequencies in this table differ from those used in the Chapman article. In addition assignments agree with those made by Mowrey et al. [14] with the exception of 643 cm^{-1} (E) and 569 cm^{-1} (T_1) where Mowrey et al. used 691 cm^{-1} (E) and 702 cm^{-1} (T_1).
[b] Units of IR activity are km/mol.

theoretical results for IR and Raman intensities, we are able to assign reported experimental IR and Raman results as shown in Tables 2–4 for P_4O_6. Computed frequencies for the HF, MP2 and DFT/B3LYP levels of calculation are shown. Infrared intensities (km/mol) and Raman intensities ($Å^4$/amu) are presented for the HF method in Table 2. MP2 and B3LYP frequency calculations yield only the IR intensities as shown in Tables 3 and 4. For an isolated P_4O_6 molecule the only allowed IR transitions are derived from vibrational modes having T_2 symmetry and the only allowed Raman transitions are from vibrational modes having A_1, E and T_2 symmetries. Note that the vibrational modes of symmetry T_1 are both IR and Raman forbidden. Also there are no vibrational modes of A_2 symmetry.

3. Scaling vibrational frequencies

There are two types of molecular motions, stretching and bending, once chemical bonds within the molecule have been established. The stretching vibration is a rhythmical movement along a bond axis. The bending vibration may consist of a change in bond angle; twisting, rocking and wagging are each specialized forms of a bending vibration.

Interpretation of an experimental IR spectrum of a complex molecule is complex. It is often built up by some "rule of thumb" empirical facts. There exists a vast compilation of such data for organic molecules [26]. For example, the CO stretching frequencies in alcohols and phenols produce a strong band in the 1260–1000 cm^{-1} region, while aliphatic aldehydes absorb near 1740–1720 cm^{-1}. The carboxylate group, $[O–C–O]^-$, has two strongly coupled C–O bond stretches giving a strong asymmetrical stretching band near 1600 cm^{-1} and a weaker symmetrical stretching band near 1400 cm^{-1}. Lack of strong absorption in the 909–650 cm^{-1} region generally indicates a non-aromatic structure. The absence of absorption in the assigned ranges for the various

Table 5
Correction factors for frequencies deduced at three levels of theory for the T_d form of P_4O_6 (the basis set used is 6-31G*)

Mode	Correction factor		
	HF	MP2	DFT/B3LYP
P–O–P wag	0.8991	0.9958	1.0221
P–O–P bend	0.8649	0.9983	1.0161
P–O stretch	0.8784	0.9746	1.0212

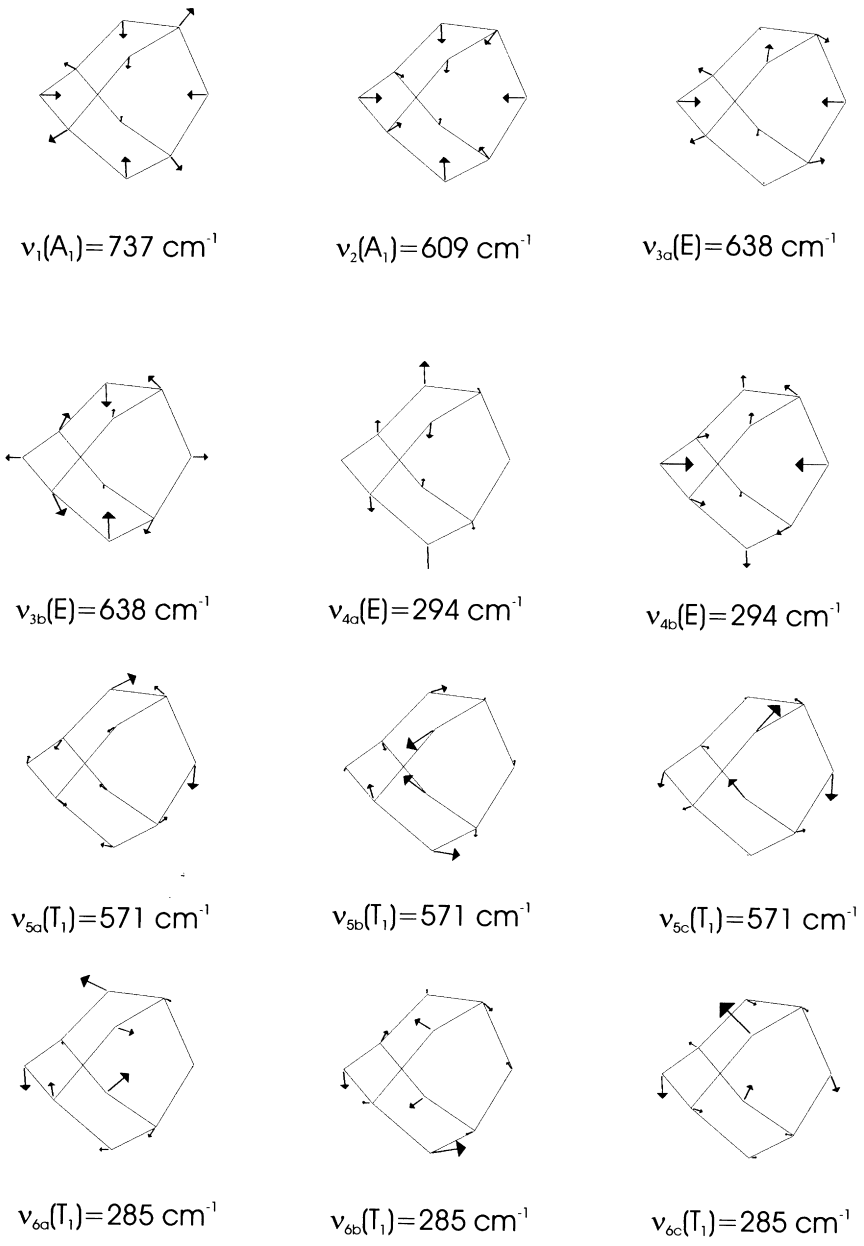

Fig. 2. Displacement vectors corresponding to the 24 normal modes of vibration of P_4O_6. The frequencies are the scaled DFT/B3LYP values that are reported in Table 4. The view is the same as used in Fig. 1.

functional groups can usually be used as evidence for the absence of such a group in the molecule.

A similar compilation of data and empirical rules for inorganic molecules would be very helpful. We have been calculating vibrational frequencies for some types of inorganic molecules for the last 10 years at different levels of the theory and comparing the results with the experimental data. Most recently studies involving P_4S_{10} [27] and P_4S_3/P_4S_7 [28] were reported. This paper is one of the series in

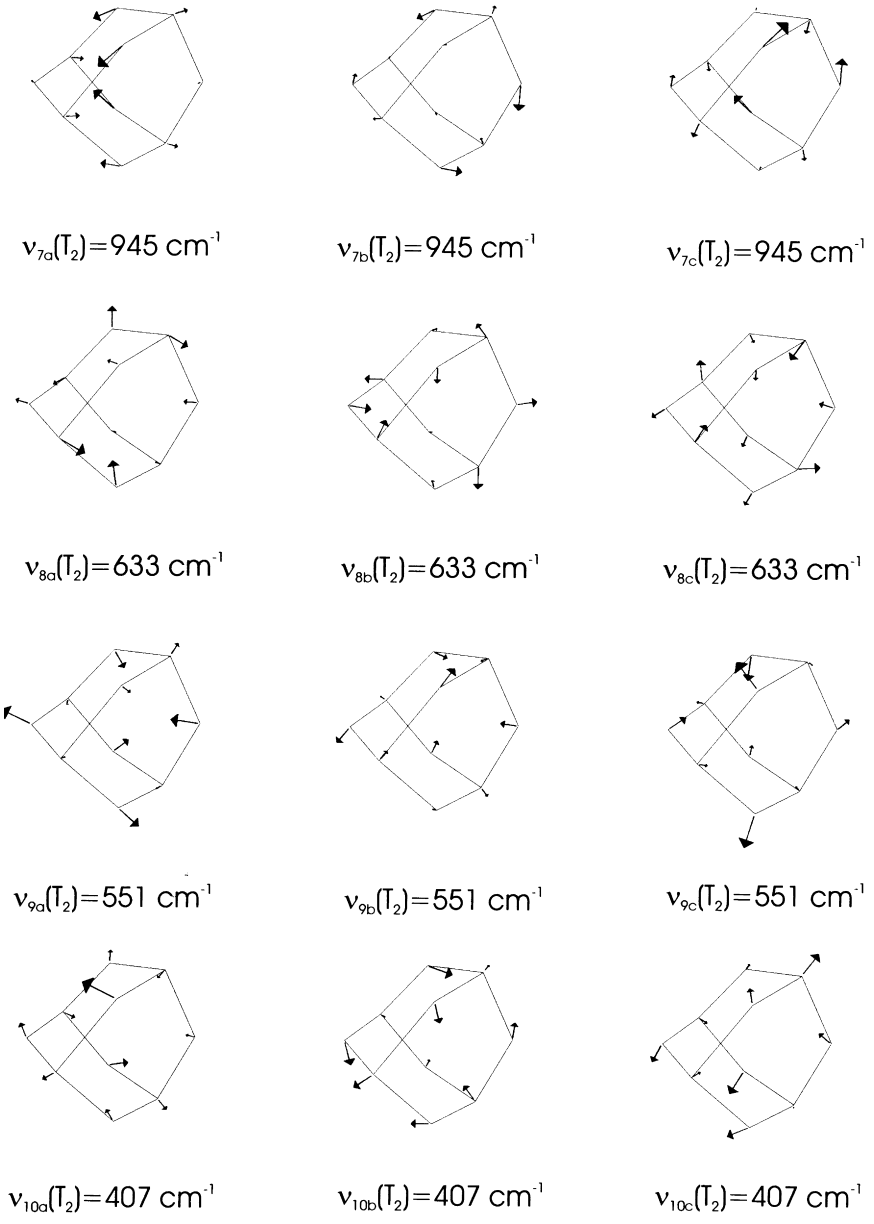

Fig. 2. (*continued*)

which we shall also undertake scaling of the computed frequencies and classify different vibrations of an inorganic molecule in terms of stretching and bending of bonds between P and O atoms in different configurations and come up with a sound scaling procedure. The aim is to perform, using the same procedure, a fair number of inorganic molecules with the hope that some trend shall emerge and be helpful to make connection between computed and observed frequencies.

Computations of vibrational frequencies at different levels of accuracy, from HF/3-21G to

MP2/6-31G* for small to moderate size molecules, H_2 to perylene ($C_{20}H_{12}$), show that the computed frequencies are generally 5–10% higher than the corresponding experimental values. Observations of empirical data shows that similar localized motions, e.g. all P–O stretches of a molecule will have a similar scaling factor (computed frequency: experimental frequency ratio). Similarly, all vibrations identifiable as P–O–P bends will have another near constant scaling factor. It is also our bias that such scaling procedures have to be essentially empirical; there are just too many complicated variables (e.g. choice of basis, Hamiltonian, and the molecular system, let alone the experimental variables) to make a reasonable causal connection. We have thus resorted to an empirical scheme, which would be simple to consistently apply without requiring too much physical intuition. Having tried out several such schemes:

(i) averaging the ratio between the experimental and computed frequencies;
(ii) minimizing the mean square error, $Q = \sum_i (\lambda\nu_{\mathrm{calc},i} - \nu_{\mathrm{expt},i})^2$; and
(iii) minimizing a weighted mean square error, $R = \sum_i w_i(\lambda\nu_{\mathrm{calc},i} - \nu_{\mathrm{expt},i})^2$, where the weight w_i, is the transition probability, chosen to be the experimental or the computational value. Whenever such weights are available, this scaling procedure yields better fits for the vibrational frequencies with higher weights.

However, based upon the criteria of simplicity and accuracy the mean square error, Q, is our final choice. Let $\{\nu_{\mathrm{expt},i}\}$ and $\{\nu_{\mathrm{calc},i}\}$, respectively, correspond to the experimental and computed frequencies for the same group of vibrations, e.g. all in the P–O stretch group. Then the computed frequencies scaled by a factor λ, be such that the mean square error, $Q = \sum_i (\lambda\nu_{\mathrm{calc},i} - \nu_{\mathrm{expt},i})^2$ be a minimum. Thus, the stationary condition $\mathrm{d}Q/\mathrm{d}\lambda = 0$, allows the determination of $\lambda = \sum_i \nu_{\mathrm{calc},i}\nu_{\mathrm{expt},i}/\sum_i (\nu_{\mathrm{calc},i})^2$. Furthermore, $\mathrm{d}^2Q/\mathrm{d}\lambda^2 = 2\sum_i (\nu_{\mathrm{calc},i})^2 > 0$, shows that this value of λ corresponds to a minimum in Q.

Based on use of the procedure proposed in Section 2, Table 5 presents a set of correction factors used for the different types of vibrational modes. These correction factors are determined by taking the average of the ratios between the computed and experimental frequencies for a particular mode, e.g. a P–O stretch. From these correction factors, the corrected frequencies are derived and presented in Tables 2–4. In these tables the quality of fitting is indicated by the root-mean-square standard deviation, $\sigma = \{\sum_i (\nu_{\mathrm{pred},i} - \nu_{\mathrm{expt},i})^2/N\}^{1/2}$ where N is the number of unique normal modes (10 for P_4O_6), which yields the following values:

HF (26 cm^{-1}), MP2 (15 cm^{-1})

and DFT/B3LYP (11 cm^{-1})

The small variation observed in these correction factors indicates that the procedure should provide reliable predictions. A vector diagram [29] for each of the 24 corrected normal modes of vibration for P_4O_6 is presented in Fig. 2.

4. Discussion

This study has considered the prediction of the normal mode vibrational frequencies and the normal mode assignments based on calculations done at the HF/6-31G*, MP2/6-31G* and DFT/B3LYP/6-31G* levels of theory. Based on use of experimentally determined normal mode frequencies, correction constants have been developed for the predominant vibrational motion in each normal mode. For P_4O_6 it is observed that the global correction factors for the 3 nonredundant motions {P–O–P wag, P–O–P bend and P–O stretch} that were considered were found to have the following ranges: HF (0.8649–0.8991), MP2 (0.9746–0.9983) and DFT/B3LYP (1.0161–1.0212). For P_4O_6 the standard deviation σ at each level of theory is found to be in the range (11–26) cm^{-1}. The fitting for DFT and MP2 are particularly worthy of note yielding σ values of 11 and 15 cm^{-1}, respectively.

Acknowledgements

We express our appreciation to The US Army Edgewood Chemical and Biological Center, US Army, for support of this work as part of the Standoff Detection Project, Project Number 1C162622A553C, Reconnaissance, Detection and Identification. The

authors also express appreciation for access to the GAUSSIAN 94 software package on the SGI Origin 2000 Computers at the Aberdeen ARL MSRC HPC.

References

[1] M.E. Fraser, D.H. Stedman, J. Chem. Soc., Faraday Trans I 79 (1983) 527–542.
[2] P.B. Davies, B.A. Thrush, Proc. R. Soc. London, Ser. A 307 (1968) 243–252.
[3] R.D. Verma, C.F. McCarthy, Can. J. Phys. 61 (1983) 1149–1159.
[4] R.J. VanZee, A.U. Khan, J. Appl. Phys. 53 (1982) 143–148.
[5] D.G. Harris, M.S. Chou, T.A. Cool, J. Chem. Phys. 82 (1985) 3502–3515.
[6] P.A. Hamilton, T.P. Murrells, J. Phys. Chem. 90 (1986) 182–185.
[7] I.H. Hillier, V.R. Saunders, Chem. Commun. (1970) 316–318.
[8] H. Gerding, H.C.J. De Decker, Recl. Trav. Chim. Pays-Bas 61 (1942) 549–560.
[9] A.C. Chapman, Spectrochim. Acta A 24 (1968) 1687–1696.
[10] I.R. Beattie, K.M.S. Livingston, G.A. Ozin, D.J. Reynolds, J. Chem. Soc. A (1970) 449–451.
[11] R.E. Egdell, M.H. Palmer, R.H. Findlay, Inorg. Chem. 19 (1980) 1314–1319.
[12] J.L. Rose, T.C. VanCott, P.N. Schatz, M.E. Boyle, M.H. Palmer, J. Phys. Chem. 93 (1989) 3504–3511.
[13] M. Mühlhäuser, B. Engels, C.M. Marian, S.D. Peyerimhoff, P.J. Bruna, M. Jansen, Angew. Chem. Int. Ed. Engl. 33 (1994) 563–565.
[14] R.C. Mowrey, B.A. Williams, J. Phys. Chem. 101 (1997) 5478–5752.
[15] L.R. Maxwell, S.B. Hendricks, L.S. Deming, J. Chem. Phys. 5 (1937) 626–637.
[16] G.C. Hampson, A.J. Stosick, J. Am. Chem. Soc. 60 (1938) 1814–1822.
[17] B. Beagley, D.W.J. Cruickshank, T.G. Hewitt, K.H. Jost, Trans. Faraday Soc. 65 (1969) 1219–1230.
[18] W.J. Hehre, L. Radom, P.v.R. Schleyer, J.A. Pople, Ab Initio Molecular Orbital Theory, Wiley, New York, 1986.
[19] C. Møller, M.S. Plesset, Phys. Rev. 46 (1934) 618–622.
[20] A.D. Becke, J. Chem. Phys. 98 (1993) 5648–5652.
[21] C. Lee, W. Yang, R.G. Parr, Phys. Rev. B 37 (1988) 785–789.
[22] GAUSSIAN 94, Revision E.1, M.J. Frisch, G.W. Trucks, H.B. Schlegel, P.M.W. Gill, B.G. Johnson, M.A. Robb, J.R. Cheeseman, T. Keith, G.A. Petersson, J.A. Montgomery, K. Raghavachari, M.A. Al-Laham, V.G. Zakrzewski, J.V. Ortiz, J.B. Foresman, J. Cioslowski, B.B. Stefanov, A. Nanayakkara, M. Challacombe, C.Y. Peng, P.Y. Ayala, W. Chen, M.W. Wong, J.L. Andres, E.S. Replogle, R. Gomperts, R.L. Martin, D.J. Fox, J.S. Binkley, D.J. Defrees, J. Baker, J.J.P. Stewart, M. Head-Gordon, C. Gonzalez, J.A. Pople, Gaussian Inc., Pittsburgh, PA, 1995.
[23] AVS-Chemistry-Viewer (Molecular Simulations Inc.,1995).
[24] GaussView 1.0 (Gaussian Inc., 1997).
[25] F.A. Cotton, Chemical Applications of Group Theory, Wiley Interscience, New York, 1971.
[26] R.M. Silverstein, G.C. Bassler, T.C. Morrill, Spectrometric Identification of Organic Compounds, 5th ed., Wiley, New York, 1991.
[27] J.O. Jensen, D. Zeroka, J. Mol. Struct. (Theochem) 487 (1999) 267–274.
[28] J.O. Jensen, D. Zeroka, A. Banerjee, J. Mol. Struct. (Theochem) (2000) (in press).
[29] A. Mukherjee, T.G. Spiro, The Svib Program: an expert system for vibrational analysis, QCPE Program 656, Indiana University, 1995.